Broadband Circularly-polarized Crossed-dipole Antenna with Good Gain Stability

Xueyan Song, Zhiyuan Wu, Xuping Li, Yunqi Zhang, and Hailong Yang

School of Electronic Engineering
Xi'an University of Posts & Telecommunications, Xi'an, 710121, China
xysong6597@126.com, 1406936884@qq.com, lixuping@163.com, johnny_5@126.com, yanghl68@163.com

Abstract – A broadband Circularly Polarized (CP) cross-dipole antenna with the merit of stable gain is proposed. The designed antenna consists of crossed dipoles, parasitic patches, reflectors, and vertical parasitic plates. By adding parasitic patches and parasitic plates, the circular polarization performance of the antenna is significantly improved. Furthermore, the gain value becomes stable in the entire operating frequency band by modifying the structure of the parasitic plates. The final dimension of the presented antenna is $0.76\lambda_0 \times 0.76\lambda_0 \times 0.28\lambda_0$ (λ_0 is the wavelength at the center frequency point in the circularly polarized working frequency band). The measured results depict that the Impedance Bandwidth (IBW) is 80.8% (2.03GHz∼4.78GHz) and the Axial Ratio Bandwidth(ARBW) is 68.5% (2.35GHz∼4.8GHz). Stable gain values, ranging from 6dBic to 7.5dBic, are obtained in the working frequency band, and the average gain can reach 7dBic.

Index Terms – broadband, circularly polarized, cross-dipole, parasitic patches, stable gain.

I. INTRODUCTION

Because of better reception performance, circularly polarized antennas have been found in many applications in Global Navigation Satellite Positioning Systems (GNSS), satellite communication systems, radio frequency identification, etc.

Microstrip patch antennas have become one of the most popular antennas due to their good characteristics, such as low profile, small size, and easy processing. Common techniques to generate CP performance are to produce a perturbation by cutting corners on the diagonal of a square patch or etching a cross slit in the ground plane. The above methods have been studied theoretically by Sharma [1] as early as 1983. The single-fed circularly polarized antenna with the perturbation method has the advantage of a simple structure. However, the bandwidth is generally narrow. In order to obtain wide circular polarization bandwidth, antennas with complementary structures, in which typically one is the crossed dipole antenna, are adopted to generate CP performance nowadays.

Due to their superior CP performance, crossed dipole antenna is one of the most popular antennas to achieve broadband and CP characteristics. In recent years, various structures of crossed-dipole antennas have been proposed to broaden the CP bandwidth. In [2], Baik proposed a crossed dipole circularly polarized antenna using a single port feed, which achieved a final ARBW of 15.6%. In [3], Baik added square opening rings to increase the ARBW of the antenna to 28.6%. By loading the butterfly-crossed dipole antenna with four parasitic triangular patches, the ARBW of the antenna in [4] can reach 42.3%. By adding circularly polarized patches, the antenna in [5] can obtain an ARBW of 66%. In [6], four grounded metal posts are inserted in the proposed antenna to achieve an ARBW of 78%. In addition, the cavity structure can also be utilized to broaden bandwidth. In [7], a surrounding non-closed cavity is formed by adding four parasitic plates, which brings about an ARBW of 63.4%. By loading a closed cavity all around, the antenna in [8] can obtain an ARBW of 58.6%. In [9], by adding folded cavity to the vertical, the ARBW of the antenna to 52.4%. In [10], in addition to the introduction of the cavity, an annular reflection ring is added between the cavity and the antenna to achieve an ARBW of 85.5%.

Although circularly polarized crossed dipole antennas own broadband property, the fluctuation of their gain values is large. The wider the bandwidth, the worse the gain flatness, as shown in Table 1. The gain flatness of the antenna is the fluctuation of gain curves in a certain band, which is an important indicator to measure the dynamic characteristics of the antenna. And the flatter the gain curve, the better the receiving characteristic of antennas. Therefore, an important parameter $\Delta G = Gain_{max} - Gain_{min}$ [12] is defined to describe the variation of gain values. To achieve stable gain, an ultra-wideband CP crossed-dipole antenna was designed in [13].

To obtain wider bandwidth and better gain flatness simultaneously, a broadband stable-gain

Submitted On: July 28, 2022
Accepted On: November 29, 2022
https://doi.org/10.13052/2022.ACES.J.371109

Table 1: Comparison of the proposed CP antenna and references

References	Overall Size (λ_0)	IBW	ARBW	Variety range of Gain (dBic)	ΔG (dB)
[5]	1.04* 1.04* 0.26	77.6% (1.11GHz -2.52 GHz)	66% (1.25GHz-2.48GHz)	7-2	5
[6]	1.17* 1.17* 0.29	95.0% (1.16GHz-3.26GHz)	85.5% (1.24GHz-3.09GHz)	1.12-6.67	5.55
[7]	0.46* 0.46* 0.1	78.3% (0.91GHz-2.08GHz)	63.4% (0.97GHz-1.87GHz)	4.5-2.5	2
[8]	0.79* 0.79* 0.27	68.9% (1.9GHz-3.9GHz)	58.6% (2.05GHz-3.75GHz)	7.4-9.4	2
[9]	0.79* 0.79* 0.27	63.2% (1.04GHz-2GHz)	52.4% (1.1GHz-1.88GHz)	2-4	2
[10]	1.1* 1.1* 0.37	98.2% (1.73GHz-5.07GHz)	85.5% (1.94GHz-4.84GHz)	6.4-10	3.6
[11]	0.6* 0.6* 0.25	44% (1.95GHz-3.05GHz)	31% (2.2GHz-3GHz)	5.8-6.5	0.7
Proposed	**0.76* 0.76* 0.28**	**80.8% (2.03GHz-4.78GHz)**	**68.5% (2.35GHz-4.8GHz)**	**6-7.5**	**1.5**

circularly polarized cross-dipole antenna is proposed in this paper. Compared with reference [13], a modified cavity is utilized in this design. The measured results show that the IBW of the proposed antenna is 80.8%(2.03GHz∼4.78GHz) and the ARBW is 68.5% (2.35GHz∼4.8GHz). And the gain flatness can keep well in the range from 6dBic to 7.5dBic.

II. ANTENNA DESIGN AND ANALYSIS

A. Antenna configuration

The physical structure of the proposed antenna is illustrated in Fig. 1. As seen from the figure, the proposed antenna is composed of three layers. In the top layer, dipole arms are printed on both sides of the F4B (ε_r=2.65, tanδ=0.001) dielectric substrate with a thickness of h, 0.8mm. Furthermore, by adding parasitic rectangular patches on both sides of the dipole arms, broad bandwidth performance can be obtained. The rectangular dipole arms are connected by a phase delay loop to achieve a 90° phase difference. The delay rings on both sides of the dielectric substrate are connected by the outer and inner conductors of a 50-ohm coaxial

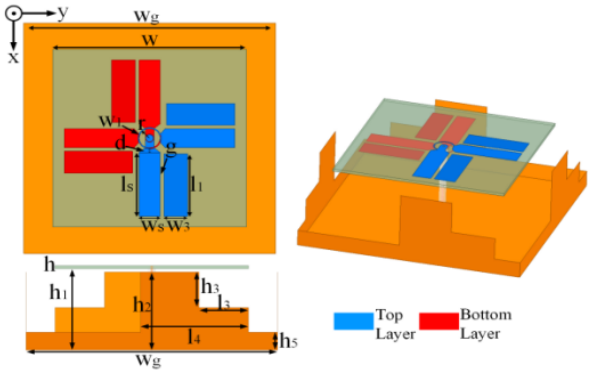

Fig. 1. The configuration of the proposed antenna.

cable. The bottom layer is mainly a metal reflector, which can further increase the gain of the antenna. Between the bottom and top layers, stepped-shaped metal walls on the vertical space are used to further broaden the bandwidth. Finally, the metal wall is modified to make the gain values stable in the entire operating band. The detailed parameter dimensions of the antenna are as follows: wg=65mm, w=50mm, r=3.2mm, w1=0.3mm, w2=2.2mm, d=1mm, ls=18mm, ws=5.4mm, g=1mm, w3=6mm, l1=17.5mm, h=0.8mm, h1=23mm, h2=22mm, h3=10mm, l3=12.8mm, l4=27.8mm, h5=5mm.

B. Design process

The proposed antenna is a crossed dipole antenna that can achieve circular polarization. The principle of the circularly polarized crossed dipole is demonstrated as follows. According to transmission line theory: $\theta = 2\pi L/\lambda$, the length of λ/4 phase delay loop is introduced in a dipole antenna. To broaden the bandwidth, parasites are added in the proposed antenna, which can produce new equivalent capacitance or inductance, thus generating different resonance points according to the resonant formula: $f = 1/(2\pi\sqrt{LC})$.

To illustrate the design process of the proposed antenna clearly, the design procedures of the proposed antenna are shown in Fig. 2. A simple crossed dipole circularly polarized antenna is designed as Ant. 1, which is evolved from the most basic crossed dipole antenna, and the bandwidth is increased by widening the dipole arm.

By adding a parasitic rectangular patch on Ant. 1, Ant. 2 is obtained, and the bandwidth is further widened caused by the generation of new resonance. Ant. 3 was generated by loading four metal walls on the vertical space between the metal plate and Ant. 2, which can bring better bandwidth performance. The vertical parasitic plate is coupled with the dipole arm, which introduces an equivalence capacitor in the low-frequency band. According to the resonance formula, the operation

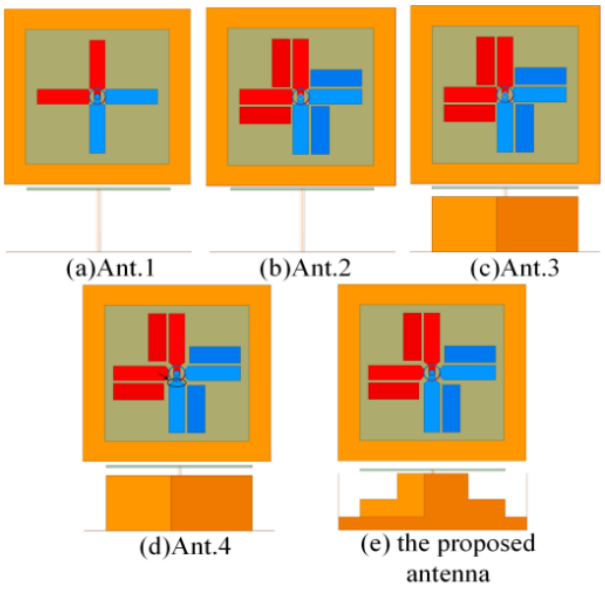

Fig. 2. Antenna evolution (a) Ant. 1, (b) Ant. 2, (c) Ant. 3, (d) Ant. 4, and (e) the proposed antenna.

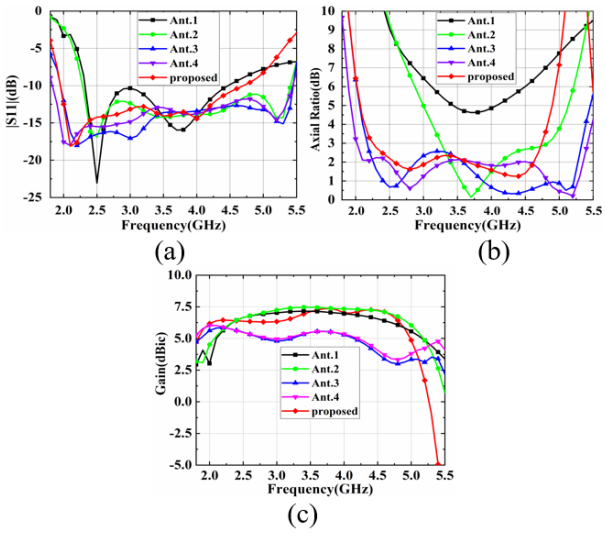

Fig. 3. Simulated results of the five antennas: (a) |S11|, (b) AR, (c) gain.

band will be expanded in low-frequency band. To further increase the bandwidth, a triangular tapering process is used between dipole arms and the phase delay loop in Ant. 3, which is present in Ant. 4. By digging rectangular notches out on the cavity structure of Ant. 4, the Ant. 5 (the proposed antenna) is obtained, the gain variation of which is slight.

C. Working mechanism

This section will illustrate the principles of wide bandwidth and gain flatness, and demonstrate the current distribution of the proposed antenna.

The simulated |S11|, AR and gain results of the above antennas are shown in Fig. 3. It can be seen from Fig. 3 that, compared with Ant. 1, Ant. 2 (loading by parasitic patches on Ant. 1) has a wider IBW of 38.6% (3.26GHz∼4.82GHz), and a wider ARBW of 81% (2.29GHz∼5.41GHz) which is because the application of the parasitic patch generates multiple resonant points. As shown in Figs. 3 (a) and (b), Ant. 2 generates a resonance point at the high frequency, and the bandwidth of |S11| and AR are widened. Then, it can also be demonstrated that the axial ratio bandwidth of Ant. 3 is broadened in both low and high-frequency band. And the ARBW can reach 81% (2.29GHz∼5.41GHz), which is because the coupling between vertical parasitic plates and dipole arms extends the current path and improves the AR in the middle and high frequencies. From Figs. 3 (a) and (b), it can be seen that the IBW of Ant. 4 is 99.3% (1.83GHz∼5.44GHz) and the ARBW of Ant. 4 is 91.4%(2.02GHz∼5.42GHz). The bandwidth is further broadened due to the improved matching by the tapering structure. Finally, in compromise of the bandwidth and gain flatness, the cavity of Ant. 5 (the proposed antenna) is designed as a stepped shape by digging out the rectangular block from the side cavity formed by the rectangular patches. Although the IBW and ARBW become narrow, the gain curves become more smooth compared with Ant. 3 and Ant. 4 as shown in Fig. 3(c). The proposed antenna exhibits an ARBW of up to 70.9% (2.26GHz∼4.71GHz) and an IBW of 82.7%. And the gain values range from 6dBic to 7.5dBic.

To clarify the cause of flatness of gain, it can be seen from the evolution from Ant. 2 to Ant. 3. Ant. 3 is constructed by adding vertical metal plates on Ant. 2, which broadens the bandwidth largely. The addition of a vertical metal plate to extend the current path by adding coupling, which moves the operation frequency band of the proposed antenna to a lower frequency band and thus broadens the bandwidth, as shown in simulation results of Ant. 2 and Ant. 3 in Fig. 3 (b) in the paper. Furthermore, the addition of a vertical metal plate mainly affects the bandwidth of antennas in the low-frequency band. While the introduction of a vertical metal plate generates coupling which makes the energy transfer to the metal plate, causing a decrease in the gain of the antenna in the high band, as can be seen from Fig. 3 (c). Additionally, the higher the frequency band, the more significant the decrease in gain. Therefore, the lower coupling is required in the high-frequency band by changing the structure of the vertical metal plate.

When the vertical metal plates are modified to stepped shapes, the coupling between the antenna and the vertical metal plate in the high-frequency band can be

decreased, which decreases the energy consumption in the high-frequency band. Therefore, the gain value in the high-frequency band becomes close to that in the low-frequency band, generating a more smooth curve of gain values.

The simulated vector surface current distribution of the proposed antenna at 2.5 GHz, 3.5 GHz, and 4.5 GHz (corresponding to the low to mid-high frequencies of the CP band) is shown in Fig. 4. It can be obtained that external parasitic components can cause resonance in the low-frequency band. As can be seen in Fig. 4 (a), the current directions at 0° and 90° are orthogonal. Therefore, the CP wave is generated. From Fig. 4 (c), the crossed-dipoles generate high-frequency resonances . As shown in Fig. 4 (b), although all antenna elements excite currents in different directions simultaneously, the overall current directions are determined in 0° and 90° directions in an orthogonal way, which brings in CP wave in the mid-frequency. Moreover, Fig. 4 also shows that the radiation at 2.5 GHz, 3.5 GHz, and 4.5 GHz is right-hand circularly polarized wave (RHCP) because the surface current flows in a counterclockwise direction at two phases.

D. Parametric analysis

Among all the parameters, the width of the vertical metal plate gap (l3) and the height of the vertical metal plate (h2) have an important effect on the performance of the presented antenna. And Fig. 5 depicts the Simulated Axial Ratio and Gain Effect of the proposed antenna with different values of l_3 and h_2. The parameter l_3 mainly affects the gain values in the high-frequency band. When l_3 increases, the coupling between the dipole arm and the metal plate reduces, which thus increases the gain values in the high-frequency band, as can be seen in Fig. 5 (a). The parameter h_2 mainly affects the AR values in the low-frequency band. When h_2 increases, the current path is extended, which generates a new resonance point and broadens the AR bandwidth in the low-frequency band, as can be seen in Fig. 5 (b).

III. SIMULATED AND MEASURED RESULTS

As shown in Fig. 6, the physical object of the proposed antenna is fabricated and measured, and Fig. 6 (c) depicts the test environment.

Shown in Fig. 7 (a) is the simulated and measured |S11| and the simulated efficiency of the proposed antenna. It can be seen that, the simulated and measured IBW (S11<-10dB) is 82.7% (1.95GHz~4.7GHz) and 80.8% (2.03GHz~4.78GHz), respectively, between which there is a deviation of 3.2% due to machining errors and losses. In addition, the measured |S11| results show a relatively large fluctuation, which is because the processing precision is insufficient, the surrounding cavity is consist of hand-folded copper pieces, and the coaxial welding is uneven. It can also be seen from Fig. 7 (a) that the efficiency of the antenna is 94% on average (the gray area in the simulated figure expresses the frequency band that the proposed antenna operates in circular polarization). Also, the efficiency of the antenna

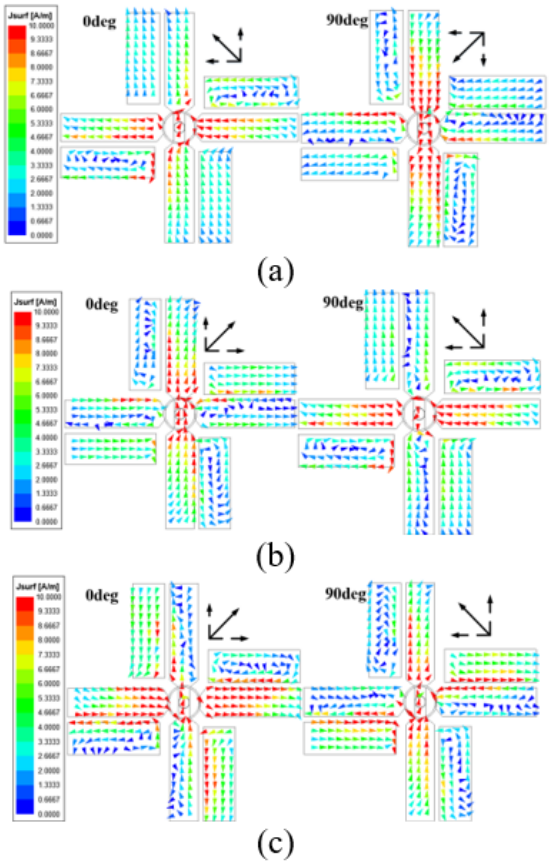

Fig. 4. The simulated surface current distribution of the proposed antenna: (a) 2.5 GHz, (b) 3.5 GHz, and (c) 4.5 GHz.

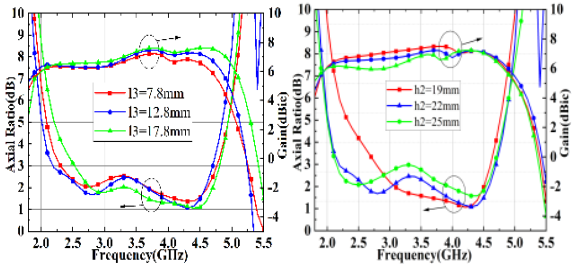

(a) (b)

Fig. 5. Simulated Axial Ratio and Gain Effect of the proposed antenna with different values of the main parameters including (a) l_3 and (b) h_2.

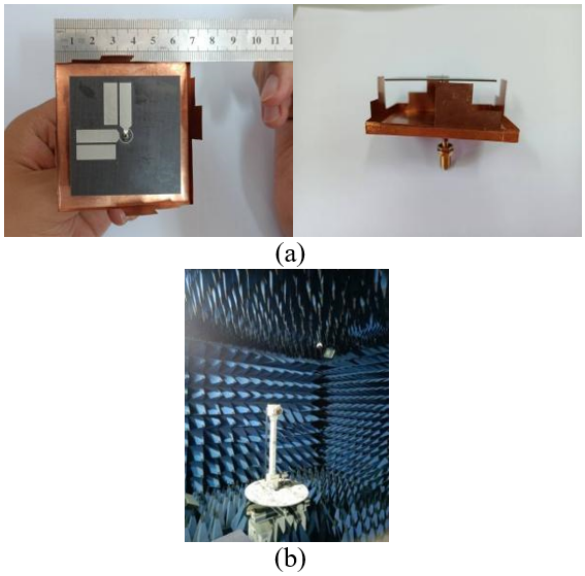

Fig. 6. (a) Photograph of the antenna. (b) The test environment.

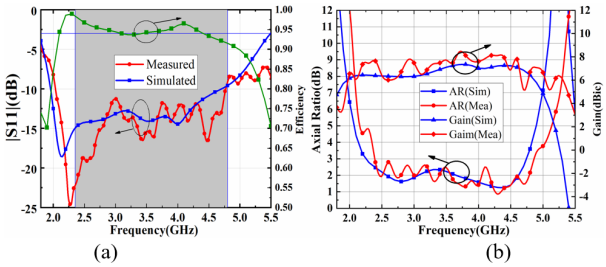

Fig. 7. Simulated and measured of (a) |S11| and efficiency (b) AR and gain.

is higher than 92% across the entire operating frequency band.

In Fig. 7 (b), the AR and gain results of the proposed antenna are depicted. The simulated and measured ARBW is 70.9% (2.26GHz∼4.71GHz) and 68.5% (2.35GHz∼4.8GHz), respectively. The simulated gain results range from 6 to 7.45dBic, and the measured gain results range from 6dBic to 8dBic, which can be seen that the average gain reaches 7dBic in the entire operating band and the gain values changes in a very small range.

The normalized radiation patterns of the proposed antenna at 2.5GHz, 3.5GHz, and 4.5 GHz (φ=0° and φ=90°) are shown in Fig. 8, from which it can be obtained that the measured radiation patterns agree well with the simulation ones, and the antenna exhibits RHCP performance in the entire CP operating band. And the measured results show that the cross-polarization of the proposed antenna is less than −15.2 dB, and the front-to-back ratio is more than 19.8 dB.

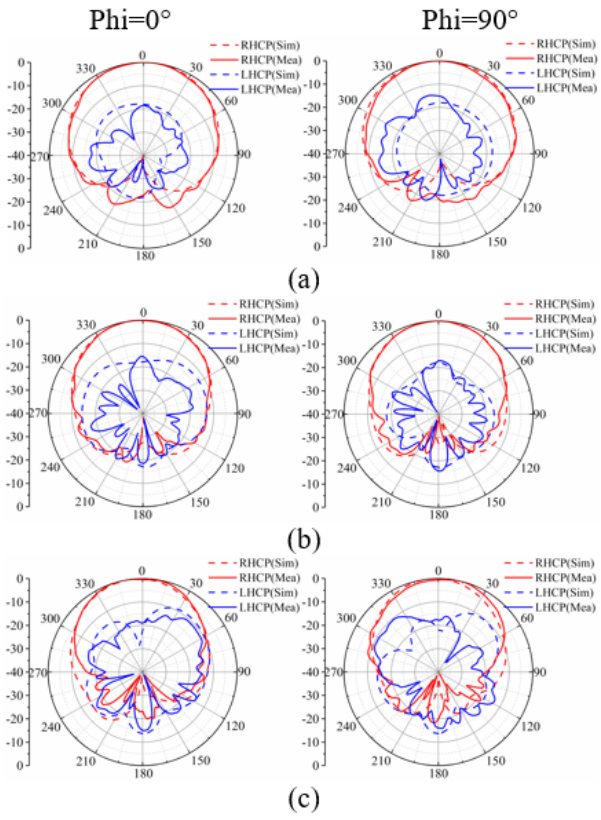

Fig. 8. Simulated and measured radiation patterns at (a) 2.5GHz, (b) 3.5GHz, and (c) 4.5 GHz.

Finally, the proposed antenna is compared with other broadband CP crossed dipole antennas in Table 1 (λ_0 is the center wavelength at the CP operating frequency in free space). Compared with antennas in [5, 7-9], the IBW and ARBW of the proposed antenna of are wider, and the gain values of the proposed antenna change slightly as seen from the minimum ΔG value of the proposed antenna. Although the IBW and ARBW of the antenna in [6] are wider than those of the proposed antenna, its overall size is larger and the variation of gain is very significant as seen from the maximum ΔG. Both the IBW and ARBW of the antenna [10] are wider than those of the proposed antenna. However, the dimension of the antenna in [10] is larger and the structure is further complicated by the addition of a circular structure between the antenna and the reflector plate, and the gain flatness is worse than that in the proposed paper. Compared with [11], the bandwidth of the proposed antenna is wider. In summary, the proposed antenna can obtain wide bandwidth and good gain flatness simultaneously.

IV. CONCLUSION

In this paper, a broadband CP crossed-dipole antenna with stable gain values is proposed. The measured results show that IBW is 80.8% (2.03GHz∼4.78GHz),

and ARBW is 68.5% (2.35GHz∼4.8GHz). By adding four improved parasitic plates, a flat gain curve of the proposed antenna is achieved in the whole frequency band, and the average gain is 7dBic. Due to the wide bandwidth and little fluctuant gain performances, the designed antenna is valuable in wireless communication systems such as indoor antennas in the frequency band of 2.4G WiFi, which requires excellent receiving characteristics. Moreover, the operation band of the proposed antenna covers parts of the 4G and 5G communication bands, which can make the designed antenna be also utilized in indoor base station communication.

ACKNOWLEDGMENT

This work is supported by the Natural Science Basic Research Program of Shaanxi (Program No. 2022JQ-699, 2022JQ-633, and 2021JQ-710) and the Key Research and Development Program of Shaanxi (Program No. 2021GY-049).

REFERENCES

[1] P. Sharma and K. Gupta, "Analysis and optimized design of single feed circularly polarized microstrip antennas," *IEEE Transactions on Antennas and Propagation*, vol. 31, no. 6, pp. 949-955, 1983.

[2] J. W. Baik, K. J. Lee, W. S. Yoon, T. H. Lee, and Y. S. Kim, "Circularly polarised printed crossed dipole antennas with broadband axial ratio," *Electronics Letters*, vol. 44, no. 13, pp. 785-786, 2008.

[3] J. W. Baik, T. H. Lee, S. Pyo, S. M. Han, J. Jeong, and Y. S. Kim, "Broadband Circularly Polarized Crossed Dipole With Parasitic Loop Resonators and Its Arrays," *IEEE Trans Antennas Propag*, vol. 59, no. 1, pp. 80-88, 2011.

[4] H. H. Tran and I. Park, "Wideband circularly polarized 2×2 antenna array with multibeam steerable capability," *IEEE Antennas and Wireless Propagation Letters*, vol. 16, pp. 345-348, 2017.

[5] L. Wang, W. X. Fang, Y. F. En, Y. Huang, W. H. Shao, and B. Yao, "Wideband circularly polarized cross-dipole antenna with parasitic elements," *IEEE Access*, vol. 7, pp. 35097-35102, 2019.

[6] Z. Zhao, Y. Li, L. Wang, Z. Tang, and Y. Yin, "Design of broadband circularly polarized antenna via loading coupled rotated dipoles," *Microwave and Optical Technology Letters*, vol. 61, pp. 425-430, 2018.

[7] W. J. Yang, Y. M. Pan, and S. Y. Zheng, "A low-profile wideband circularly polarized crossed-dipole antenna with wide axial-ratio and gain beamwidths," *IEEE Transactions on Antennas and Propagation*, vol. 66, no. 7, pp. 3346-3353, 2018.

[8] H. H. Tran, I. Park, and T. K. Nguyen, "Circularly polarized bandwidth-enhanced crossed dipole antenna with a simple single parasitic element," *IEEE Antennas and Wireless Propagation Letters*, vol. 16, pp. 1776-1779, 2017.

[9] H. Zhang, Y. Guo, and G. Wang, "A design of wideband circularly polarized antenna with stable phase center over the whole GNSS bands," *IEEE Antennas and Wireless Propagation Letters*, vol. 18, no. 12, pp. 2746-2750, 2019.

[10] Y. Feng, J. Li, B. Cao, J. Liu, G. Yang, and D. Wei, "Cavity-backed broadband circularly polarized cross-dipole antenna," *IEEE Antennas and Wireless Propagation Letters*, vol. 18, no. 12, pp. 2681-2685, 2019.

[11] M. Sefid, C. Ghobadi, and J. Nourinia, "Broadband circularly polarized crossed-dipole antenna and its array for long-term evolution communication systems," *International Journal of RF and Microwave Computer-Aided Engineering*, vol. 31, no. 12, e22896, 2021.

[12] Y. Chen, S. Wang, S. Shi, M. Jiang, J. Ding, J. Gao, and G. Zhai, "Landstorfer Printed Log-Periodic Dipole Array Antenna With Enhanced Stable High Gain for 5G Communication," *IEEE Transactions on Antennas and Propagation*, vol. 69, no. 12, pp. 8407-8414, 2021.

[13] Z. Wu, X. Li, and X. Song, "An improved ultra-wideband circularly polarized cross-dipole antenna," *13th International Symposium on Antennas, Propagation and EM Theory (ISAPE)*, pp. 1-3, 2021.

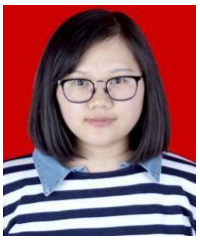

Xueyan Song was born in Henan Province, China, in 1989. She received her B.E. degree in electronic and information engineering from Xidian University, Xi'an, China, in 2012. She received a Ph.D. degree in Electromagnetic Fields and Microwave Technology from Xidian University, Xi'an, China, in 2018.

She joined the School of Electronic Engineering, Xi'an University of Posts and Telecommunications in 2018. Her research interests include artificial magnetic conductors, low RCS antennas, low-profile antennas, frequency-selective surfaces, and reflector antennas.

Zhiyuan Wu was born in Hubei Province, China, in 1995. He is currently pursuing a Master of Engineering degree in the School of Electronic Engineering, Xi'an University of Posts and Telecommunications. His current research interests include circularly polarized antennas, metamaterials, and array antennas.

Xuping Li was born in Xi'an, Shanxi, China in 1981. He received a Ph.D. degree in electromagnetic fields and microwave technology from Xidian University, Xi'an, China, in 2015. His research interests are antenna theory and engineering.

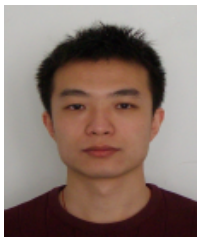

Yunqi Zhang was born in BaoTou, Inner Mongolia, China. He received a Ph.D. degree from Xidian University, Xi'an, China in 2015. He is currently working at the Xi'an University of Posts & Telecommunications. In 2017 he joined the School of Physics and Optoelectronic Engineering at Xidian University, as a postdoctoral candidate. His research interests include GPS antenna, CP antenna, omnidirectional antenna, and antenna array designs.

Hailong Yang received a B.S. in Communication Engineering from Heze University, Heze, China, in 2012. He earned M.S. and Ph.D. degrees in Communication Engineering from Xi'an University of Technology, Xi'an, China, in 2015 and 2019, respectively. He joined the faculty of the Electronic Engineering Department, Xi'an University of Posts and Telecommunications, in 2019. His research interests include wave propagation and antenna design.